AN IMPROVED TWO-LOOP BEAM ENERGY STABILIZER FOR AN FN TANDEM ACCELERATOR*

Thomas A. Trainor
University of Washington Nuclear Physics Laboratory
Seattle, Washington 98195 USA

Introduction

This article describes a two-loop regulator for an electrostatic accelerator which maintains the beam position at the image slit of the 90° energy-analyzing magnet stable to a degree equivalent to a 100 volt rms fluctuation of the terminal voltage. The regulator is relatively simple to set up and has very good recovery from tank sparks and beam interruptions. This permits long-term operation without the need for attention by experimentors or staff. Individual elements of the two-loop regulator are described in turn, followed by a discussion of the regulator system as a whole. Finally, the relationship between transfer functions for the two loops required for best operation is presented.

Corona Discharge Regulator

This is a fundamental element of most regulation systems for electrostatic accelerators. Its chief advantage is a large control range. For a typical corona current range of 100 μA (6BK4) and column resistance of ∿30GΩ (FN tandem) the corresponding terminal voltage swing permitted is 3 MV. The principle disadvantage of a corona regulator is the sharp cutoff in frequency response above about 10 Hz.

In fig. 1 is shown the measured open-loop frequency response and phase shift for an FN tandem corona regulator. The measurement was made by exciting the corona triode grid with an audio oscillator and observing the resulting signal on a capacitive pickup with a lock-in amplifier. Use of the lock-in enabled the measurements to be extended to the interesting region above 10 Hz. Corrections have been made for intervening reactive elements.

Not shown on this figure is an inferred first RC corner at about 0.06 Hz due to the terminal-tank capacitance. Rolloff proceeds from this corner at 20 db/decade (-90°) up to about 10 Hz. In this region the finite flight time of negative ions to the terminal along the corona discharge comes into play. The flight-time effect produces the series of minima and maxima with a further general rolloff at 20 db/decade resulting in an effective overall rolloff of 40 db/decade for the maxima. Also in this region the open-loop phase shift departs rapidly from -90° until finally the phase becomes meaningless at frequencies above ∿80 Hz due to the statistical nature of the ion transport.

A stability requirement for a servo loop such as the corona regulator is that at all frequencies for which the open-loop gain is greater than unity the accumulated phase shift around the loop must be less than 180° (in fact, less than 180° by a phase margin of 20°-40° in practical systems). Inspection of fig. 1 indicates that unity gain for the corona loop is fixed at or below 10-15 Hz in the best case and varies somewhat depending on terminal voltage, corona points position and tank gas pressure.

*Work supported in part by the U. S. Department of Energy.

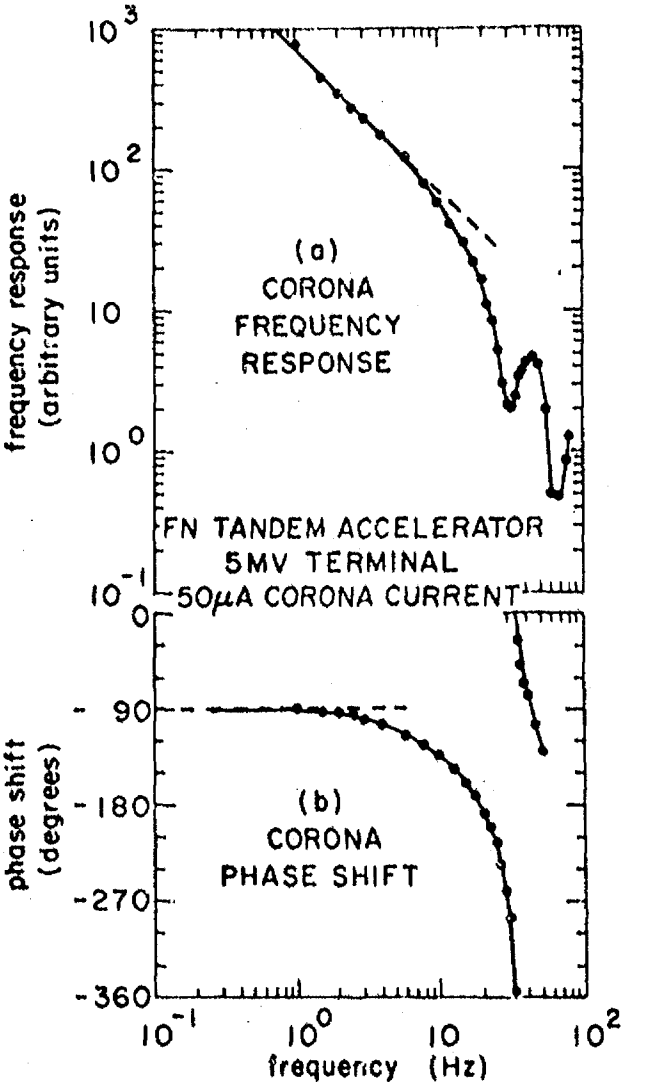

Fig. 1 Corona regulator frequency response (a) and phase shift (b)

With this limitation in mind how much residual terminal voltage noise do we expect with a single corona regulator loop? The terminal voltage noise spectrum consists of long term drifts of order 100-500 kV, decreasing as 1/f at higher frequencies and roughly proportional to average terminal voltage. At a fundamental frequency of 2.5 Hz and harmonics the charging belt contributes a discrete spectrum of voltage noise with an rms value near 10 kV and somewhat independent of terminal voltage. If the gain of the corona loop is fixed at unity at 10 Hz the gain is 6 at 2.5 Hz and about 200 below the first corner at 0.06 Hz. The residual terminal voltage noise will therefore be 1-2 kV as typically observed. For precision work, or in situations where because of a malfunction the voltage noise is unusually large, additional noise reduction gain must be achieved. This is possible with an additional fast voltage control loop.

Stripper Voltage Regulator

One of the first fast loops was installed in the University of Washington tandem in 1972. It consists of a high-voltage amplifier in the terminal which drives the foil or gas stripper. The amplifier input is derived from an axial IR light link consisting of an LED, photo transistor and simple large aperture optical system.

Installation of this fast loop or "terminal regulator" resulted in improved energy resolution and reduced beam intensity modulation. The resulting two-loop system was operated as installed until 1979 when it was decided to overhaul the regulator system by eliminating ground loops, combining separate control panels and investigating the fundamental limitations of the two-loop system.

The analysis of the corona loop was described above. A similar analysis of the stripper loop as originally installed revealed that the frequency response was that of two successive low-pass RC stages with corners at 450 Hz and 1.5 kHz. Because there were two stages of integration the fast loop accumulated a total phase shift of -180° above about 2 kHz. A very poor feature of this regulation loop was the proximity of the two corner frequencies, resulting in a maximum stable gain of 4 flat from DC to about 400 Hz. Furthermore, because the fast loop response extended to DC the stripper power supply, with a range of 4 kV, was forced to "compete" with the corona discharge to correct voltage errors of hundreds of kV, thus sending the fast loop into saturation for a significant fraction of the time.

Remedial action was determined as follows. Unity gain for the fast loop was established at about 1.5 kHz, since this second corner frequency (due to the stripper-to-stripper box capacitance) was fixed by a hardware geometry. Maximum gain for this loop was required at the charging belt fundamental, 2.5 Hz. Therefore, a passive lag filter was inserted in the loop which moved the corner at 450 Hz down to 5 Hz. Also included was a passive high-pass RC stage with corner at 1.2 Hz. The resulting open-loop gain (shown as G_S in fig. 7) has a maximum at 2.5 Hz and rolls off smoothly at 20 db/decade down to DC and up to 1.5 kHz where the second corner occurs. The maximum possible loop gain (at 2.5 Hz) is now 500 and the behavior at low frequency is most compatible with operation of the corona loop as discussed below.

Logarithmic Slit Preamplifiers

The best source of information available about terminal voltage fluctuations is the fluctuation of momentum-analyzed beam current on the image slit jaws. In order to achieve good fidelity in conveying this information to other elements of the control loops the image slit current preamplifiers must be logarithmic to provide the best common mode rejection of beam current fluctuations. They must be low noise units, both in the sense of fast ambient noise and in terms of thermal drifts. They must be fast, in the sense that the frequency response is flat from DC to beyond the 1.5 kHz corner in the stripper loop. And, the preamplifiers should have a uniform logarithmic response over a broad current range from less than 100 pA to more than 10 μA.

The slit preamplifier circuit shown in fig. 2 is adapted from a system used to determine semiconductor parameters. It is temperature compensated, has a 1V/decade gain curve (within 3%) from 10 pA to 100 μA and has separate feedback loops for capacitance and temperature compensation.

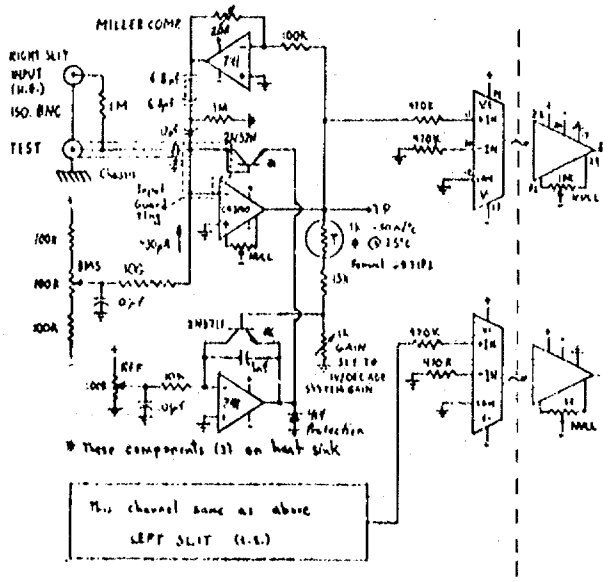

Fig. 2 Logarithmic Slit Preamplifier

The capacitance compensation action can be seen in fig. 3. In (a) a 1nA square wave on a 10nA background is fed into the log preamp with minimum compensation. The square wave is being integrated by stray capacitance in the transdiode element of the preamp. This integration becomes very serious at currents below about 10 nA, since the effective resistance involved is derived from the slope of the log characteristic. In (b) the gain in the compensation loop is properly adjusted for best rise time (~100 μs) without ringing.

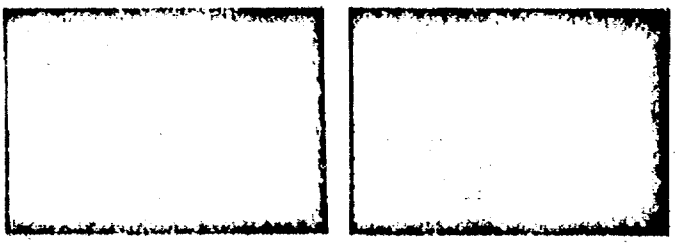

Fig. 3 Log preamplifier performance without (a) and with (b) capacitance compensation (200 μs/div.)

In addition to the compensation above it is very important that ground loops be eliminated and capacitive coupling to AC sources be minimized. In this circuit opto isolators are used, a single point ground is made to the beam drift tube, and shrouds have been placed around the slit jaw adjustment micrometers to shield the slit cooling access holes. A closed-circuit oil cooling system for the slits has been installed to eliminate current leakage, acoustical noise, and static charge buildup noise. The preamps themselves are placed in a double-shielded box also containing a double-shielded power supply transformer enclosed in μ-metal, and special low-noise coaxial cable is used between the slits and the preamp inputs.

This combination of steps has resulted in a total line frequency and acoustical rms noise current equivalent to loss than 10 pA.

An additional source of "noise" is secondary electron cross talk between slits. We have staggered the image slits 20 cm apart symmetrically about the image point of the analyzing magnet, and each slit has its own biased suppression cage within the drift tube. This system has eliminated all secondary electron problems.

The performance of the slit preamps is shown in fig. 4. In (a) the difference and sum signals are shown with beam present. The beam has been purposefully adjusted to produce a significant intensity modulation, illustrating the excellent common mode rejection capability of the slit preamps. This good common mode rejection is only possible if the amplifier gains are matched at all frequencies out to 2 kHz. This means that the capacitance compensation, as well as the DC gains, must be matched. The difference signal in (a) is equivalent to a total equivalent voltage fluctuation of about 100 volts. The fast fluctuations in the signal are derived from 800 Hz ripple in the terminal high voltage power supply. In (b) there is no beam on the slits and the residual line and acoustical noise can be seen.

Fig. 4 Slit current difference (top) and sum (bottom) signals for beam on (a) and off (b) (200 mV/div. (a), 50 mV/div. (b), 50 ms/div.)

Beam Energy Controller

The unified control system which evolved during this project is shown as a block diagram in fig. 5. There are three analog inputs: the slit current difference signal (~1V/kV) the slit current sum signal (1V/decade) and the GVM signal (1V/MV, this also drives analog and digital meters on the control console). The slit sum signal is compared to an adjustable level to provide error signals interior to the energy controller and also to the data acquisition system.

An external unit called the Terminal Voltage Experiment Control (TVEC) can be used to put a digital window on the GVM signal. A TTL signal indicating the presence of the terminal voltage within this window is provided both to the beam energy controller and to the data acquisition system.

There are two analog outputs. The grid signal for the corona triode (6BK4) has a range of ± 10 V, and the current output to the fast-loop LED varies from 0-100 mA consistent with the diode rating. The corona triode output is protected by back-to-back zener diodes against high voltage transients which occur during a tank spark.

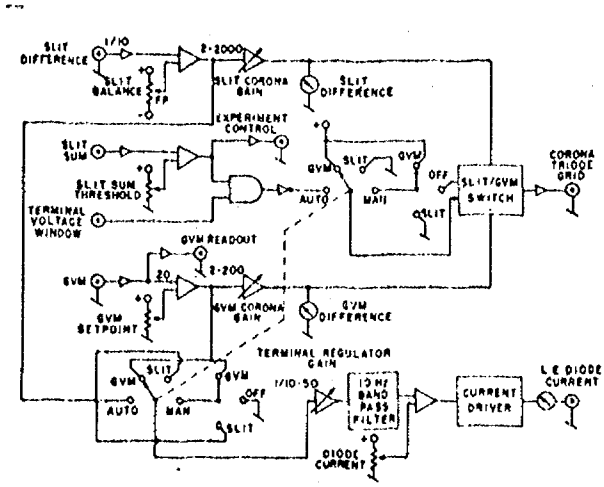

Fig. 5 Beam energy stabilizer block diagram

Choice of signal source for either control device is made with a four-position rotary MODE switch. In the GVM or SLIT mode both control devices (corona, stripper) use a single signal source. In MANual mode either signal source may be chosen for either control device by means of toggle switches. This is most useful during initial adjustment. These switches may also be used to turn off or open either control loop. In the AUTO mode the stripper loop uses the image slit difference as a signal source, and the corona loop follows the GVM error signal unless the TVEC signal is true (terminal voltage within window) and the slit current sum signal is above the preset threshold, in which case the system automatically switches to slit control for the corona loop. This twofold condition for slit control of the corona loop provides excellent control recovery from tank sparks or beam interruptions, especially for heavy ion beams, in contrast to the requirement on minimum slit current alone which permits control on unwanted ion species with the same magnetic rigidity at lower (or higher) terminal voltages.

Separate corona loop gains are provided for SLIT and GVM difference signals. The diode loop has a common gain for both signals since it is not switched in AUTO operation. The DC component of the diode current is separately adjusted so that voltage excursions of the stripper high voltage supply occur over its linear output range. Improper adjustment of this parameter is indicated by clipping of the diode current when the stripper supply saturates.

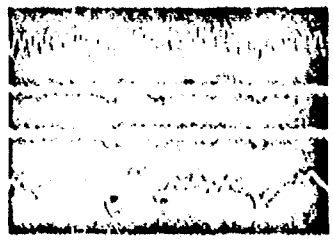

Fig. 6 Voltage regulator inputs and outputs: Top-slit sum (500 mV/div.), second-slit difference (500 mV/div.), third-corona grid (10 V/div.), bottom-LED current (all 50 ms/div.)

Fig. 6 shows simultaneously the inputs and outputs of the voltage regulator system operating in slit control. One can see a 60 Hz ripple on the slit sum signal due to position modulations on the object slits. The slit difference signal is equivalent to a 100 V rms terminal voltage fluctuation. The corona loop has received a gain factor of 20 within the control circuitry, but the total DC open loop gain is almost 10,000 for this figure. The diode current is shown at bottom with a stripper open loop gain of about 200. With this gain the diode current accurately depicts the residual voltage noise on the terminal after corona stabilization.

Two-loop Transfer Functions

For a single servo loop with open-loop gain G the noise reduction factor is $(1+G)^{-1}$. Limitations on G have been cited above in the section on the corona regulator. For that case the maximum DC gain is typically about 200. If a second loop is introduced the interplay of the two must be properly described.

Let V_T and V_S be the differential excursions in the terminal and stripper voltages. Then $V=V_T+V_S$ is the differential excursion in the effective accelerating potential. The noise reduction factor for the terminal voltage V_T with both control loops operating is

$$[1 + \frac{G_C}{1+G_S}]^{-1} = [1 + G_T]^{-1}$$

and that for the effective accelerating potential V is

$$[1 + G_C + G_S]^{-1} = [1 + G_V]^{-1}$$

where G_C and G_S are the corona and stripper open-loop gains. Fig. 7 shows a composite of the various factors. The corona loop gain G_C (shown with a DC gain of 10,000) is as shown in fig. 1. With this DC gain the corona loop alone would be violently unstable, with large oscillations at about 15 Hz. However, addition of the stripper loop makes G_T the effective noise reduction gain for V_T, and it is G_T, not G_C, which must satisfy the servo stability criterion.

It is easy to see that the high-pass element at the stripper loop filter acts to stabilize the terminal. Because G_S is increasing at 20 db/decade in the denominator of G_T below 1 Hz G_T decreases at almost 40 db/decade from 10,000 at DC to unity gain at 15 Hz, as required for stability of the composite system. The DC stability of the terminal voltage is therefore excellent, but the charging belt noise at 2.5 Hz and above is about the same as with the single corona loop.

The beam energy is now determined by the effective acceleration potential V, and the corresponding noise reduction gain G_V falls smoothly at 20 db/decade from 10,000 at 0.1 Hz to unity at 1 kHz. For a typical noise spectrum this results in a residual rms noise less than 100 V over the complete frequency range of interest.

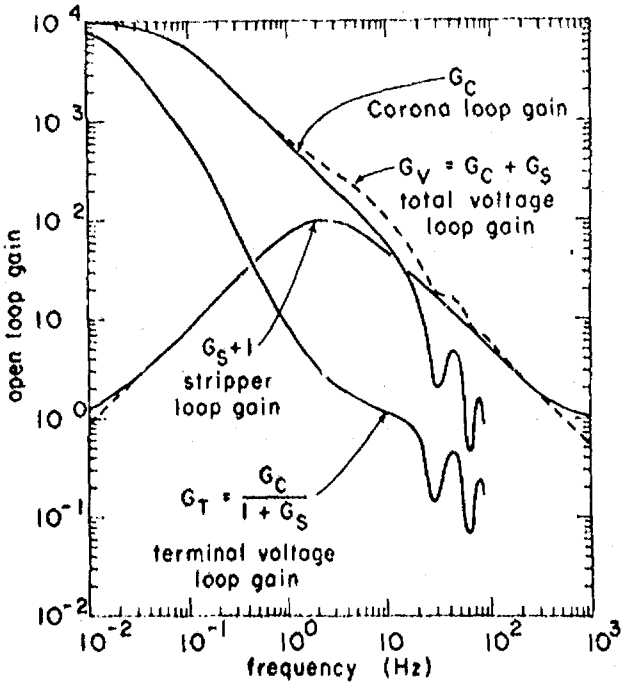

Fig. 7 Energy regulator transfer functions

Summary

By performing a detailed analysis of the properties of various elements in a two-loop voltage regulator for a tandem accelerator we have been able to design an "optimum" system which reduces effective accelerating voltage noise below 100 V. Essential features of the new system are high-quality slit preamplifiers, careful attention to removal of extraneous noise sources, and proper shaping of frequency responses to maximize stable gains and insure compatibility of the two control loops. The resultant beam energy stabilizer system is easy to operate, has well defined indicators for proper adjustment of operating parameters, and recovers reliably from beam interruptions.